An Investigation on Collapse Behavior of Shear Localization in Elasto-Thermo-Viscoplastic Materials

Hyun-Gyu Kim*
Department of Mechanical Engineering, Seoul National University of Technology, 172 Gongneung-2dong, Nowon-gu, Seoul 139-743, Korea
Seyoung Im
Department of Mechanical Engineering, Korea Advanced Institute of Science and Technology, Science Town, Taejon 305-701, Korea

The stress collapse in the formation of shear bands in elasto-thermo-viscoplatic materials is systematically studied within the framework of one-dimensional formulation via analytical and numerical methods. The elastic energy released in a domain is found to play an important role in the collapse behavior of shear localization. A non-dimensional parameter named the stability indicator is introduced to characterize the collapse behavior, with approximate forms of the incremental governing equations. The stability indicator offers useful information regarding the degree of severity of an abrupt change of deformations during the stress collapse. Numerical experiments are carried out to verify the stability indicator by varying material properties.

Key Words : Shear Localization, Shear Band, Instability, Stress Collapse, Elastic Unloading

1. Introduction

The shear localization into a narrow band develops in a variety of materials, and plays an important role in the damage mechanism under impact loading conditions. Inhomogeneous deformations originating from impurities, imperfections, wave propagation, and other sources begin to grow, and ultimately a critical condition for localization is reached. There have been extensive researches using computational and analytical methods on this subject.

Machand and Duffy (1988) presented that there exist three stages of deformations : homogeneous deformation, followed by the stress collapse wherein shear localization develops into a narrow band, and finally, a post-localization state or fully-developed state. At the time of the stress collapse, the intensive localization of the plastic deformation into a shear band may accompany an abrupt change of the plastic strain rate. The strong stress drop may cause a loss of stability in numerical calculations. Needleman (1988) has shown that there is a numerical instability during the stress collapse if a band width is discretized into several elements to simulate the shear localization in a viscoplastic material. Batra and Kim (1990) also obtained unstable solutions during the stress collapse in examining the simple shear deformations in thermo-viscoplastic materials, taking fine mesh near the band region, even though they used a higher order method such as the Gear method. Although a number of researches have been made in experimental, theoretical and numerical investigations on shear localization, there is still a lack of understanding of how material properties combine to the behavior of the stress collapse in the formation of shear bands.

The purpose of the present study is to understand the mechanism of the stress collapse of

* Corresponding Author,
E-mail : khg@snut.ac.kr
TEL : +82-2-970-6309; **FAX** : +82-2-949-1458
Department of Mechanical Engineering, Seoul National University of Technology, 172 Gongneung-2dong, Nowon-gu, Seoul 139-743, Korea. (Manuscript **Received** August 7, 2006; **Revised** September 8, 2006)

shear localization and to explore the role of material properties in relation to the behavior during the stress collapse. We start from the energy balance of a system of shear localization for one-dimensional simple shear deformation under a constant velocity at the boundary. We introduce the energy-balance number to explain the collapse behavior of shear localization. This non-dimensional number turns out to be useful for explaining a highly strong drop of the stress and a dramatic increase of the plastic strain rate in a shear band. As a key expression, we propose a dimensionless parameter consisting of material properties and boundary velocity, named the stability indicator. Despite its underlying assumptions, the stability indicator shows very good performances in characterizing the behavior of shear localization during the stress collapse. As the stability indicator approaches a limit value, an enormously large plastic strain rate occurs, and the governing equations become extremely stiff. We also address important material properties associated with the degree of severity of the stress collapse, and illustrate the collapse behavior according to the values of the stability indicator.

2. Stress Collapse of Shear Localization

The detailed processes of the formation of shear localization are very complicated with thermo-mechanical coupling and micro-structural change in metals. Three stages of deformations in the development of shear bands, appearing in the torsional Hopkinson bar test, are clearly observed: the growth of inhomogeneous deformations, the stress collapse, and the post-collapse state. Here we focus on the stress collapse, which occurs when the nominal strain reaches a critical value.

In general, the shear localization process has the nature of being one-dimensional in a body, and the analysis with the simple shear deformation can capture many important features of shear localization. Accordingly, we analyze the simple shear deformation of an infinite plane strain slab with finite height $2L$, as shown in Fig. 1. Note that the velocity V_0 is prescribed on the top and

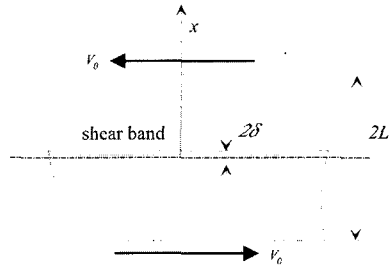

Fig. 1 One-dimensional simple model for the analysis of shear band

the bottom surfaces of the block. The non-zero components of stress and strain are only shear terms, which are the functions of time t and the vertical coordinate x. The governing equations for the balances of linear momentum and energy in the one-dimensional problem are written as

$$\rho\frac{\partial v}{\partial t}=\frac{\partial \tau}{\partial x},\ 0\le x\le L \tag{1}$$

$$\rho c\frac{\partial \theta}{\partial t}=k\frac{\partial^2\theta}{\partial x^2}+\kappa\tau\dot{\gamma}^p,\ 0\le x\le L \tag{2}$$

In the above equations, the field variables are the velocity v, the stress τ, the plastic strain rate $\dot{\gamma}^p$, and the temperature θ. The material parameters ρ, c, k and κ denote the density, the specific heat, the thermal conductivity, and the coefficient of converting plastic work into thermal energy, respectively. In the present study, we consider the following types of elasto-thermo-viscoplastic materials:

$$\dot{\tau}=\mu\dot{\gamma}^e \text{ with } \dot{\gamma}^e=\dot{\gamma}-\dot{\gamma}^p \tag{3}$$

$$\dot{\gamma}^p=f(\tau,\gamma^p,\theta) \tag{4}$$

where μ is the shear modulus, $\dot{\gamma}^e$ and $\dot{\gamma}$ are the elastic and total strain rates, respectively, and the dot denotes the differentiation with respect to time.

2.1 Energy balance during the stress collapse

During the stress collapse in the formation of shear bands, the energy balance neglecting the kinetic energy due to the inertia leads to the following relation:

$$P_{appl}+P_{elas}=P_{diss} \tag{5}$$

where P_{appl} is the applied power at the boundary, P_{elas} is the rate of the elastic energy released in the domain, and P_{diss} is the dissipation rate of energy in shear bands. When the stress falls down strongly, the elastic unloading power P_{elas} may be much larger than the applied power P_{appl}. For this case, a large amount of input power from the elastic energy released in the domain is concentrated on shear bands as the dissipation power. As a result, a very narrow shear band should absorb a large amount of the dissipation power when the stress falls down strongly. Since the stress is only a function of time in Eq. (1) in the absence of the inertia, we can then define the following non-dimensional parameter ξ such that

$$\xi=\frac{P_{elas}}{P_{diss}}=(-)\frac{\tau L\dot{\tau}/\mu}{\int_0^L \tau\dot{\gamma}^p\,dx} \tag{6}$$

We call ξ the energy-balance number. From the relation described in Eq. (5), it follows that the energy-balance number ξ for the problem under the constant velocity at the boundary, neglecting the inertia, cannot be larger than one.

We first consider the release of unloading elastic energy during the stress collapse for the simple shear model given in Fig. 1, wherein the shear band width is 2δ. Here, we assume a constant velocity V_0 imposed at the upper and the lower boundaries. Since the plastic strain rate outside the shear band is nearly zero during the stress collapse, the constitutive equations inside and outside the shear band may be assumed to take the following different forms:

$$\dot{\tau}=\mu(\dot{\gamma}-\dot{\gamma}^p) \text{ for } |x|<\delta \tag{7a}$$

$$\dot{\tau}=\mu\dot{\gamma} \text{ for } |x|>\delta \tag{7b}$$

From the velocity boundary condition, we can obtain the compatibility condition

$$\int_0^\delta \dot{\gamma}\,dx+\int_\delta^L \dot{\gamma}\,dx=V_0 \tag{8}$$

Substituting the constitutive equation outside the shear band into Eq. (8) gives

$$\int_0^\delta \dot{\gamma}\,dx=V_0-(L-\delta)\frac{\dot{\tau}}{\mu} \tag{9}$$

Integrating Eq. (7a) and applying Eq. (9), the following expression is obtained:

$$\int_0^\delta \dot{\gamma}^p\,dx=V_0-L\frac{\dot{\tau}}{\mu} \tag{10}$$

The last term on the right-hand side of Eq. (10) corresponds to the velocity at the boundary from the elastic strain rate. Therefore, we see that the applied power on the boundary and the elastic power released throughout the domain are concentrated on the shear band in the form of plastic work, as both sides of Eq. (10) are multiplied by the stress τ. An excessively large amount of elastic energy released during the stress collapse may give rise to an extremely large value of the plastic strain rate inside the shear band, together with an abrupt collapse of the stress. As a result, the system of shear localization exhibits an extremely stiff behavior as ξ in Eq. (6) approaches one.

If the shear modulus μ is large and the stress drop rate $\dot{\tau}$ is not too severe, the velocity from the elastic strain rate, given by the second term in Eq. (10), may be much smaller than the prescribed velocity V_0. For this case, Eq. (10) can be approximated by

$$\int_0^\delta \dot{\gamma}^p\,dx\approx V_0 \tag{11}$$

In the post-localization regime, the stress rate is small under the velocity boundary condition, and the above approximation is valid. For thermo-viscoplastic materials, the relation between the width of the shear band and the maximum plastic strain rate can be obtained from this approximation (Wright, 1987; Kim and Im, 1999).

2.2 Approximate analysis of the collapse behavior

Our aim here is to introduce a dimensionless parameter indicative of the collapse behavior of shear localization in terms of material properties and boundary velocity. To obtain a complete and exact solution to the problem of shear banding seems impossible because of the non-linearity of the governing equations. However, the major features of the collapse behavior of shear localization can be observed by taking a linearization and a simplification of the governing equations.

As mentioned before, we neglect the inertia in the equation of motion, and consider the aforementioned simple shear deformation under the prescribed velocity V_0. We examine the incremental equilibrium right after the onset of shear localization, of which the major mechanism is thermal softening. Making a simplification in Eq. (10) such that the distribution of the plastic strain rate inside the shear band is uniform, we can write the incremental form as

$$\Delta\tau=\mu\frac{V_0}{L}\Delta t-\mu\frac{\delta}{L}\Delta\gamma^p \tag{12}$$

where Δ means the incremental operator. The simplified incremental equation includes the compatibility for the velocity at the boundary as well as the relaxation of stress due to the plastic flow in the shear band.

The heat diffusion at the early time of the stress collapse does not take up a large portion in the energy equation (Glimm et al., 1996; DiLellio and Olmstead, 1997). Hence, we shall disregard the heat diffusion in the energy equation, and then following incremental equation after the onset of shear localization is obtained:

$$\rho c\Delta\theta\approx\kappa\tau_0(1+b\dot{\gamma}^p)^m(1-\alpha\theta)\Delta\gamma^p \tag{13}$$

We restrict our attention, for illustration, to the following specific form of the flow rule, based on Litonski's flow rule (Litonski, 1977), in the absence of strain hardening effects:

$$\tau=\tau_0(1+b\dot{\gamma}^p)^m(1-\alpha\theta) \tag{14}$$

where α, b, m, and τ_0 are the material parameters. The strain hardening is usually neglected in comparison with the strain rate hardening as the plastic strain increases dramatically for metals (Merzer, 1982). We therefore restrict ourselves to the flow rule without the strain hardening, and this simplification will hardly make a difference regarding the basic physics of the thermo-mechanical deformation during the stress collapse. The strain rate hardening parameter m is very small in most metals, and the temperature increment grows linearly with the plastic strain increment as shown in Eq. (13). As a result, the incremental form of the flow rule is approximately written as

Table 1 Reference material properties

Properties	Symbols	Values
Density	ρ	7860.0 kg/m^3
Specific heat	c	473.0 J/kgK
Thermal conductivity	k	49.2 W/mK
Dissipation factor	κ	1.0
Shear modulus	μ	8.0×10^{10} N/m^2
Reference shear stress	τ_0	6.02×10^{8} N/m^2
Strain rate sensitivity	m	0.0251
Reference strain rate	b^{-1}	1.0×10^{-4}s^{-1}
Softening coefficient	α	$6.43\times10^{-4}K^{-1}$

$$\Delta\tau\approx(-)\alpha\tau_0(1+b\dot{\gamma}^p)^m\Delta\theta \tag{15}$$

Eq. (15) means that the thermal softening has more significant contribution to the stress collapse than the strain rate hardening.

We want to find a simple approximation for the relations described in Eqs. (13), (14) and (15), which represent the incremental quantities right after the onset of shear localization. Generally, the plastic strain rate $\dot{\gamma}^p$ at the beginning of the stress collapse has a similar value to the nominal strain rate V_0/L. Hence, we take $(bV_0/L)^m$ for a representative value of $(1+b\dot{\gamma}^p)^m$ due to $b\dot{\gamma}^p\gg1$ (see Table 1). Moreover, for the sake of simplicity, we neglect the $(1-\alpha\theta)$ term in Eq. (14) because the temperature is not high at the beginning of the stress collapse, based upon $\alpha\theta\ll1$. This simplification minimizes the nonlinearity of the constitutive equation to facilitate the illustration of the underlying mechanism of shear localization. Accordingly, Eqs. (13) and (15) become

$$\Delta\tau\approx(-)\frac{\alpha\kappa\tau_0^2(bV_0/L)^{2m}}{\rho c}\Delta\gamma^p \tag{16}$$

The numerical results will justify these approximations in that a non-dimensional parameter from Eq. (16) provides a good indication for the collapse behavior of shear localization. Combining Eqs. (12) and (16) gives the following relations:

$$\frac{\Delta\gamma^p}{\Delta t}=\left(\frac{1}{1-\bar{\xi}^*}\right)\frac{V_0}{\delta} \tag{17}$$

$$\frac{\Delta\tau}{\Delta t}=(-)\mu\left(\frac{\bar{\xi}^*}{1-\bar{\xi}^*}\right)\frac{V_0}{L} \tag{18}$$

$$\bar{\xi}^*=\frac{\kappa\alpha(bV_0/L)^{2m}\tau_0^2L}{\rho c\delta\mu} \tag{19}$$

A meaningful solution to Eqs. (12) and (16) is only possible when $\bar{\xi}^*<1$ so that the plastic strain rate inside the shear band remains a finite value. Ultimately, for $\bar{\xi}^*=1$, there will be no bounded solution to Eqs. (12) and (16). In this case, the jumps in γ^p and τ or the infinite values of $\dot{\gamma}^p$ and $\dot{\tau}$ near the critical time are apparent from Eqs. (17) and (18).

We now turn our attention to the physical interpretation of the dimensionless parameter $\bar{\xi}^*$. Multiplying the numerator and the denominator of $\bar{\xi}^*$ by $\Delta\theta$ in Eq. (19), we see from Eqs. (14), (16) and (19) that $\bar{\xi}^*$ is nothing but the ratio of the portion converted into heat out of the elastic energy $(-)\tau L\Delta\tau/\mu$ released in the domain to the heat energy $\rho c\delta\Delta\theta$ that the shear band can absorb. Noting that $\rho c\delta\Delta\theta/\kappa$ is just the dissipation increment while $\alpha\Delta\theta(bV_0/L)^{2m}\tau_0^2L/\mu$ indicates the elastic energy released in the domain, we see that $\bar{\xi}^*$ has the same interpretation as ξ.

The stress collapse starts from the shear band region, and the unloading wave propagates to the boundary region in the presence of the inertia, so that the unloading occurs sequentially from the center to the boundary. Therefore, the elastic energy release rate for this sequential stress collapse is less than the value of the no-inertia case wherein the stress collapse occurs almost instantaneously throughout the domain. Furthermore, the applied energy at the boundary and the unloading elastic energy are converted into the kinetic energy over the entire domain as well as the dissipation energy inside shear bands. For a short time, the unloading waves with elastic wave speed travel back and forth between the boundary and the center, and the stress and the plastic strain rate at the center may oscillate.

In the finite element computation, the consequence of the aforementioned observation is linked to the mesh dependence during the stress collapse. The maximum plastic strain rate $\dot{\gamma}^p$ of a FEM solution is determined from the resolution capacity of a finite element mesh when $\dot{\gamma}^p$ increases to an extremely large value. A large value of $\dot{\gamma}^p$ will be obtained, as the finite element model is discretized into a finer mesh for not small values of $\bar{\xi}^*$. In this case, the shear band is too thin, and a fine refinement enough to capture the steep deformation across the shear band is required. When the mesh is discretized further as $\bar{\xi}^*$ approaches 1, we may encounter numerical instability or ill-conditioning in finding the solution due to the deformation approaching a highly stiff behavior with an extremely large plastic strain rate $\dot{\gamma}^p$. For coarse meshes, which are not fine enough to represent a narrow shear band or a large $\dot{\gamma}^p$, this numerical instability may be avoided, but the instability mode becomes diffusive and filtered out.

As in the aforementioned discussion, the expression for $\bar{\xi}^*$ may provide information regarding the degree of severity of the instability during the stress collapse. However, $\bar{\xi}^*$ itself involves the thickness δ of the shear band. It would be very informative and desirable to have a dimensionless parameter like $\bar{\xi}^*$ in terms of material properties and boundary velocity only. The half band width δ in Eq. (19) may be determined by material properties and boundary velocity, but it is not easy to find the band width at the onset of localization. However, numerical experiments (see Fig. 7) show that the band width at the critical time is approximately proportional to the value at the post-collapse stage. Batra and Chen (2001) showed the dependence of the band width with the drop of the shear stress in the formation of shear band. The half band width at the post state was proposed by Kim and Im (1999) such that

$$\delta_{post}\approx\cosh^{-1}(2G-1)\frac{mk}{\kappa\alpha(bV_0/L)^m\tau_0V_0} \tag{20}$$

where G is the constant. Accordingly, we replace the shear band width δ in Eq. (20) by δ_{post} in Eq. (20) for establishing a non-dimensional parameter in terms of material properties and boundary velocity. Dropping off the constant term $\cosh^{-1}(2G-1)$ in Eq. (20), we may define

the following dimensionless number.

$$\bar{\xi}=\frac{\kappa^2\alpha^2(bV_0/L)^{3m}\tau_0^3LV_0}{\rho cmk\mu} \tag{21}$$

We call $\bar{\xi}$ the stability indicator. Note that $\bar{\xi}$ does not take the same value as ξ or $\bar{\xi}^*$ because of approximations made so far. If $\bar{\xi}$ approaches a limit value $\bar{\xi}_l$ that corresponds to $\xi\rightarrow 1$, extremely stiff changes of the stress and the plastic strain rate may occur. It may be impossible to carry out numerical computations passing the stress collapse for $\bar{\xi}$ close to $\bar{\xi}_l$ unless the mesh is coarse enough to filter out the instability mode. There are many parameters in Eq. (21) involved in the stability of shear localization. First of all, the elasticity plays an important role in association with the collapse behavior, as manifested by the fact that the stability indicator $\bar{\xi}$ approaches zero as the shear modulus μ goes to infinity or the material becomes rigid-viscoplastic. The changes of the reference shear stress τ_0 and the thermal softening coefficient α have a prominent influence upon the collapse behavior of shear localization, as evidenced by Eq. (21). Larger stability indicator is achieved as the density ρ, the specific heat c, the strain rate sensitivity m and the conductivity k decrease. DiLellio and Olmstead (2003) showed that the OFHC copper does not exibit the dramatic drop in shear stress associated with the formation of a shear band. On the contrary, they observed a strong stress drop and oscillations of the plastic strain rate for the case of the 4340 steel. The reason of different behaviors for these materials is that the OFHC copper has much smaller value of the stability indicator compared to the 4340 steel.

3. Numerical Experiments

In numerical calculations of the shear localization in elasto-thermo-viscoplastic materials, the stability of the numerical scheme is an important consideration. Hence, we simultaneously solve the coupled equations with a proper updating scheme for the state variables instead of the staggered algorithm in which the mechanical field variables are fixed during the calculation of the thermal field. The trapezoidal scheme is chosen for integrating the energy equation while the iterative backward Euler scheme (Lush et al., 1989) is used for updating the state variables in the viscoplastic constitutive equation.

We use the flow rule given in Eq. (14) for the one-dimensional simple model with height $L=3.47\times10^{-3}$ m, and the reference material properties are listed in Table 1. In numerical experiments, the material properties are varied to investigate the collapse behavior of shear localization. In order to facilitate the initiation of localization, we assume a small perturbation of the initial temperature at the center. The initial temperature perturbations in terms of the non-dimensional variable $\hat{x}$ are given as follows:

$$\hat{\theta}(\hat{x},0)=0.1[1-(\hat{x})^2]^9e^{-5(\hat{x})^2} \tag{22}$$

The time for the onset of shear localization is known to be dependent upon the size of the initial perturbations (Wright and Walter, 1987).

All finite elements for the displacement and the temperature fields have linear polynomials for interpolation, and the one point integration rule is employed. To obtain a highly refined mesh in one-dimensional problems near the center region wherein the localization occurs, we construct the finite element mesh according to the following equation

$$x_i=\left(\frac{i-1}{N}\right)^{\gamma}L,\ 1\le i\le N+1 \tag{23}$$

where N is the total number of elements, and γ is the refinement index.

3.1 Collapse behavior

In this section, numerical simulations are carried out to examine the development of the shear band depending upon the energy-balance number ξ, the stability indicator $\bar{\xi}$, and the mesh refinement. To observe the behaviors of numerical solutions, we vary the shear modulus μ, associated with the rate of elastic energy released in the domain. In order to exclude the influence of the inertia from the numerical solutions in relation to the energy-balance number and the mesh refinement, we neglect the inertia term in these analyses. The constant velocity $V_0/L=15000$ 1/s

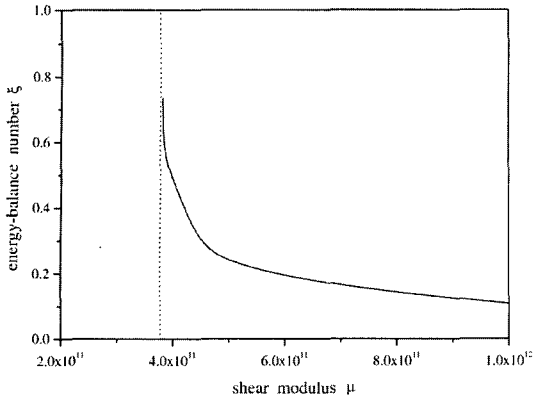

Fig. 2 Energy-balance number ξ versus the shear modulus μ; dotted line is the limit shear modulus in numerical computations

is prescribed at the boundary, and the results are presented in Fig. 2. As the shear modulus μ decreases, the energy-balance number ξ given in Eq. (6) approaches 1.0. As a consequence, numerical solutions for ξ approaching 1 show an extremely stiff behavior accompanying a large plastic strain rate inside a very narrow band as the mesh is refined.

The material properties in Table 1 are utilized to define the reference value $\bar{\xi}_{ref}$ of the stability indicator. In the numerical analyses to follow, three cases are calculated depending upon the stability indicator $\bar{\xi}$: this reference value, 1/10 times and 1/100 times the reference value. The last two values of the stability indicators are obtained by taking 10 times and 100 times the reference shear modulus, respectively. As evidenced later (see Fig. 6), the conclusions to follow remain unchanged even though $\bar{\xi}$ is adjusted by changing the other properties like α, τ_0, ρ, etc. instead of μ, i.e. the consequences remain the same regardless of how $\bar{\xi}$ is set up. We take the mesh refinement according to the refinement index r in Eq. (23).

To examine the behaviors of the numerical solutions depending upon the mesh refinement and the stability indicator $\bar{\xi}$, we obtain the plot of the plastic strain rate $\dot{\gamma}^p$ versus the nominal strain $\bar{\gamma}$, and the plot of the stress τ versus $\bar{\gamma}$ for the aforementioned three stability indicators and for different mesh refinements. Note that the

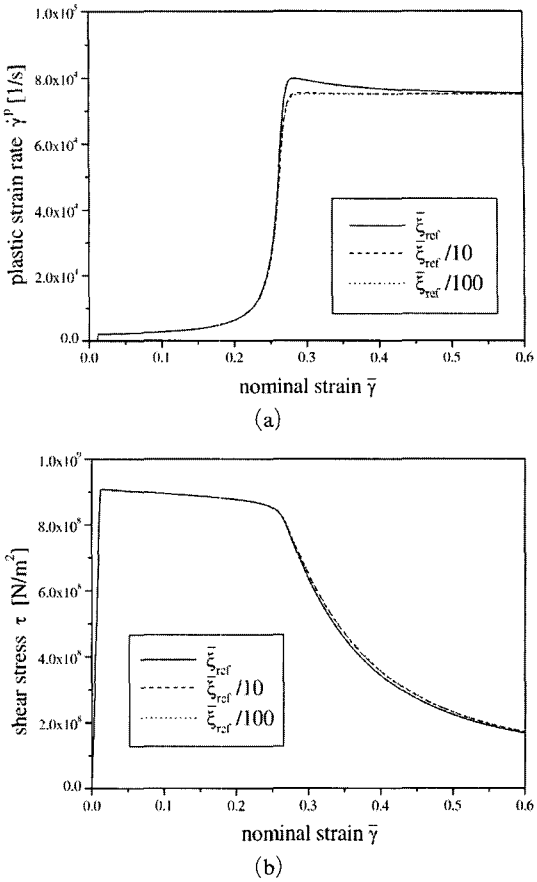

Fig. 3 Numerical results for three stability indicators when mesh refinement index r is 1.0; (a) plastic strain rate; (b) stress in the first element

nominal strain $\bar{\gamma}$ is a time parameter, and the plastic strain rate $\dot{\gamma}^p$ and the stress τ on the plot have been computed on the element closest to the specimen center ($x=0$). Fig. 3 through Fig. 5 show the plastic strain rate and the shear stress versus the nominal strain for the mesh refinement index $r=1.0$, $r=1.5$, and $r=2.0$, respectively. As seen in Fig. 3(a), only a minor overshoot of $\dot{\gamma}^p$ is obtained for $r=1.0$ at $\bar{\xi}=\bar{\xi}_{ref}$, which is the reference stability indicator. On the other hand, a large overshoot of $\dot{\gamma}^p$ is observed at $\bar{\xi}=\bar{\xi}_{ref}$ for $r=1.5$ and $r=2.0$, as seen in Figs. 4(a) and 5(a). In the coarse mesh of $r=1.0$, the deformation in the shear band is smeared into one large element, which results from the uniform spacing, and the genuine shear localization is not cap-

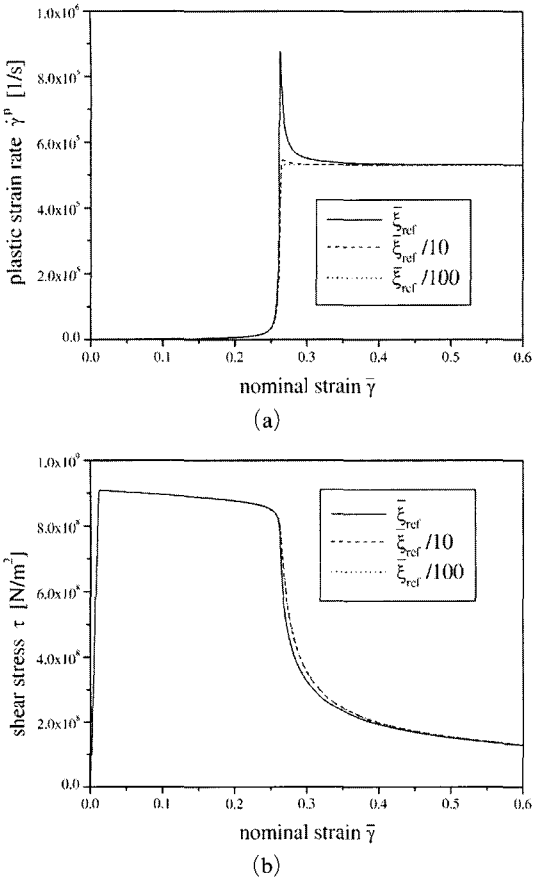

Fig. 4 Numerical results for three stability indicators when mesh refinement index r is 1.5; (a) plastic strain rate; (b) stress in the first element

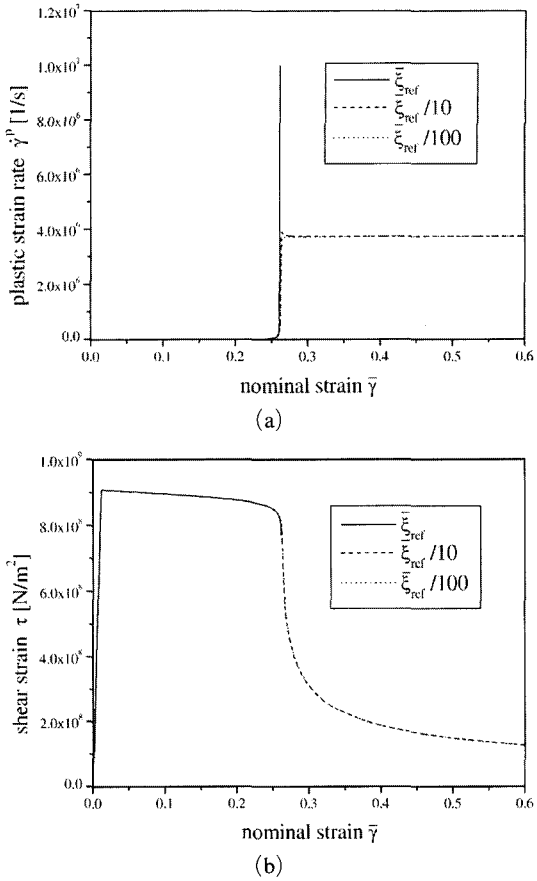

Fig. 5 Numerical results for three stability indicators when mesh refinement index r is 2.0; (a) plastic strain rate; (b) stress in the first element

tured. As the finite element refinement proceeds, the numerical solutions show an increasingly large overshoot of the plastic strain rate $\dot{\gamma}^p$ for $\bar{\xi}=\bar{\xi}_{ref}$, and they tend to capture the shear localization. For $r=2.0$, the numerical instability was encountered for $\bar{\xi}=\bar{\xi}_{ref}$, and the computation could proceed no longer (see Fig. 5). As discussed in Section 2.1, this implies that an excessive elastic energy released in the domain is concentrated into a narrow shear band during a strong stress collapse. As a consequence of this, the plastic strain rate in the shear band increases to an extremely large value, and the time step required in numerical computation becomes too short to cover a practically meaningful span of deformations. However, there are no difficulties in numerical computations for the lower values of $\bar{\xi}$, i.e. $\bar{\xi}=\bar{\xi}_{ref}/10$ and $\bar{\xi}=\bar{\xi}_{ref}/100$, as shown in Figs. 5(a) and 5(b). We can obtain the numerical solutions with fine mesh of $r=2.0$ for these lower values of the stability indicators.

We now verify the stability indicator with regard to the variation of material properties. We examine whether or not the numerical instability occurs, for varying values of material properties, at the same value of the stability indicator $\bar{\xi}=\bar{\xi}_l$, which indicates the limit value of $\bar{\xi}$ wherein the numerical instability occurs first for a sufficiently small time step ($\Delta t=1.0\times10^{-10}$) and a fine mesh ($r=5.0$). A very small time step and fine mesh are essential for removing the dependency of the instability occurrence on the time step and mesh.

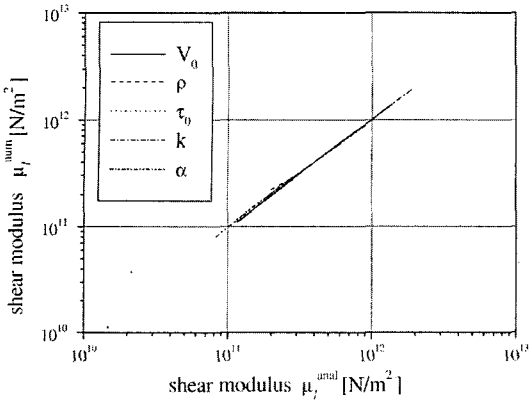

Fig. 6 Comparison of limit shear moduli μ_l^{num} and μ_l^{anal} obtained by numerical calculations and by Eq. (21), respectively, to give the limit value $\bar{\xi}_l=3.24$ according to the changes of material properties

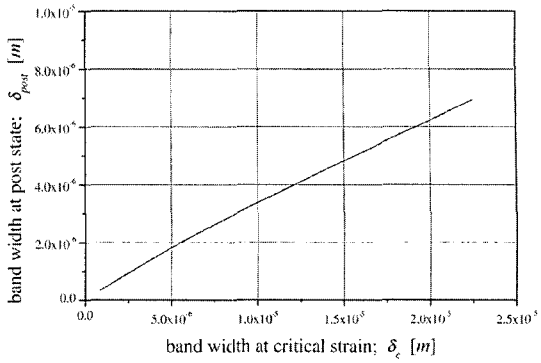

Fig. 7 Relation between shear band widths at the critical strain and at the post state

The limit shear moduli μ_l^{anal} are calculated in accordance with Eq. (21) corresponding to the limit stability indicator $\bar{\xi}_l=3.24$ in numerical computations. This limit stability indicator has been computed, employing the material data in Table 1 and decreasing the shear modulus gradually until the numerical instability is first encountered. On the other hand, the limit shear moduli μ_l^{num} that lead to numerical instability with the sufficiently fine mesh ($r=5.0$) and the small time step ($\Delta t=1.0\times10^{-10}$) are obtained. The comparisons of μ_l^{anal} and μ_l^{num} are plotted versus the variation of material properties in Fig. 6. The two shear moduli μ_l^{anal} and μ_l^{num} show an excellent consistency with each other with respect to the variation of material properties — the boundary velocity V_0, the density ρ, the reference shear stress τ_0, the thermal conductivity k, and the coefficient of thermal softening α. This confirms the fact that the stability indicator $\bar{\xi}$ characterizes the collapse behavior of shear localization very well. Furthermore, the justification for replacing the band width in Eq. (19) by Eq. (20) is shown by Fig. 7, in which the band width at the critical strain is approximately proportional to the value at the post-collapse state. The critical strain is defined by the time of the maximum change of the plastic strain rate in the shear band. Note that the boundary of the shear band is defined to be the one-tenth valued point of the plastic strain rate at the center. Taken together, we conclude that Eq. (21) provides a good indicator for the collapse behavior of shear localization in elasto-thermo-viscoplastic materials.

As discussed in Section 2, near $\bar{\xi}=1$ there may occur a dramatic change in $\dot{\gamma}^p$ and τ with regard to the time parameter $\bar{\gamma}$. Such a tendency at the critical strain accompanies the mesh-dependence of the numerical solution and the abrupt decrease of the width of the shear band. The regions of numerical stability and instability, depending upon the smallest element size and the stability indicator $\bar{\xi}$, are presented together with $\bar{\xi}_l$ in Fig. 8. It is noted that the region of stability for numerical solution is enlarged as the smallest element size increases beyond the half band width δ_{post} of the post stage because the shear band is smeared into one large element. This implies that stable computation is possible even beyond the limit stability indicator $\bar{\xi}_l$, though it fails to lead to an accurate solution near the shear band when the finite element mesh is coarse enough to cause the smearing of the shear localization. However, there is no change in the size of the two regions or in the critical value of the stability indicator as the element size becomes sufficiently small below δ_{post}.

3.2 Inertia

As previously mentioned, the behavior during the stress collapse without the inertia cannot be calculated by numerical methods if the stability

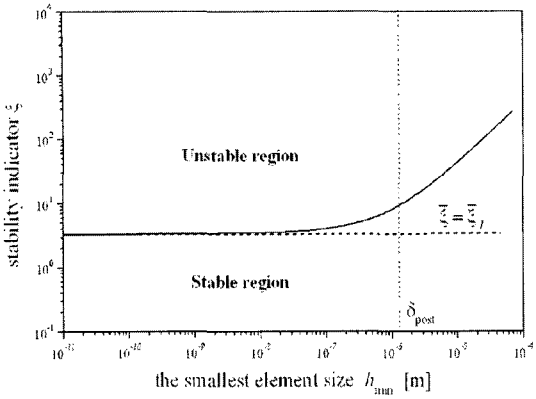

Fig. 8 Stability indicator in numerical computations with varying mesh refinements

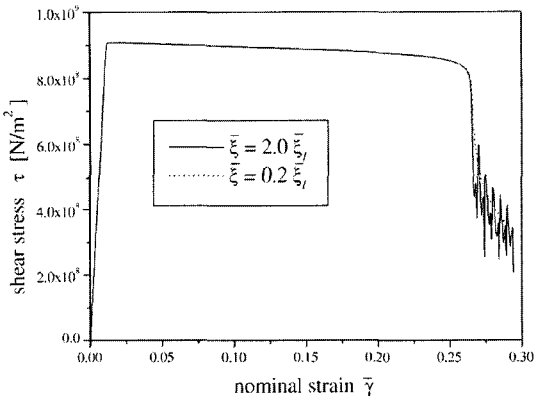

Fig. 9 The stress at the center for $\bar{\xi}=2.0\bar{\xi}_l$ and $\bar{\xi}=0.0\bar{\xi}_l$ as a function of the nominal strain when the inertia term is included in numerical computations

indicator $\bar{\xi}$ is larger than the limit value. However, the stabilizing effect of the inertia may alleviate this difficulty because the stress falls sequentially from the center to the boundary, and the kinetic energy absorbs the elastic unloading energy. In Fig. 9, the numerical calculations for $\bar{\xi}=2.0\bar{\xi}_l$ and $r=5.0$, which lead to the numerical instability for the no-inertia case, pass the critical strain and produce a severe oscillation during the stress collapse when the inertia term is taken into account. The oscillatory behaviors of the plastic strain rate and the stress after the onset of shear localization have been also reported by Fressengeas (1989). This is due to the rebound of the unloading wave at the boundary when the inertia term absorbs a large amount of the elastic energy released in the domain. On the contrary, there is no oscillation for the lower stability indicator $\bar{\xi}=0.2\bar{\xi}_l$ (see Fig. 9). For a small value of $\bar{\xi}$, -elatively small unloading elastic energy released in the domain does not yield oscillatory behaviors during the stress collapse.

4. Conclusions

The formation of shear bands was investigated with a view to exploring the behavior of stress collapse of shear localization in elasto-thermo-viscoplastic materials. We explain the collapse behavior in terms of the energy-balance number, which is the ratio of the rate of the unloading elastic energy released to the rate of the energy dissipated in a shear band. From a simplified model, the stability indicator $\bar{\xi}$ is introduced in order to gain an insight into the effects of material properties on the collapse behavior, carrying a meaning similar to the energy-balance number ξ. The energy-balance number and the stability indicator play important roles in understanding computational difficulties during the stress collapse in the development of shear bands. The governing equations become extremely stiff when the energy-balance number ξ approaches one, and an extremely large plastic strain rate is observed inside the shear band during the stress collapse.

Although simplifications are made to develop the stability indicator $\bar{\xi}$, the validity of this non-dimensional parameter expressed by material properties and boundary velocity was verified through a series of numerical experiments. We addressed material properties which have a significant effect on the collapse behavior of shear localization. Moreover, the mesh refinement was explained in conjunction with the stability indicator ξ.

References

Batra, R. C. and Chen, L., 2001, "Effect of Viscoplastic Relations on the Instability Strain, Shear Band Initiation Strain, the Strain Corresponding to the Minimum Shear Band Spacing, and the Band Width in a Thermoviscoplastic Ma-

terial," *International Journal of Plasticity*, Vol. 17, pp. 1465~1489.

Batra, R. C. and Kim, C. H., 1990, "Effect of Integration Methods on the Solution of an Adiabatic Shear Banding Problem," *International Journal for Numerical Methods in Engineering*, Vol. 29, pp. 1639~1652.

DiLellio, J. A. and Olmstead, W. E., 1997, "Temporal Evolution of Shear Band Thickness," *Journal of the Mechanics and Physics of Solids*, Vol.45, pp. 345~359.

DiLellio, J. A. and Olmstead, W. E., 2003, "Numerical Solution of Shear Localization in Johnson-Cook Materials," *Mechanics of Materials*, Vol. 35, pp. 571~580.

Fressengeas, C., 1989, "Adiabatic Shear Morphology at Very High Strain Rates," *International Journal of Impact Engineering*, Vol. 8, pp. 141~157.

Glimm, J. G., Plohr, B. J. and Sharp, D. H., 1996, "Tracking of Shear Bands I. The One-dimensional Case," *Mechanics of Materials*, Vol. 24, pp. 31~41.

Kim, H. G. and Im, S., 1999, "Approximate Analysis of a Shear Band in a Thermoviscoplastic Material," *ASME Journal of Applied Mechanics*, Vol. 66, pp. 687~694.

Litonski, J., 1977, "Plastic Flow of a Tube under Adiabatic Torsion," *Bulletin Acad. Polymer Sciences*, Vol. 25, pp. 7~14.

Lush, A. M., Weber, G. and Anand, L., 1989, "An Implicit Time-integration Procedure for a Set of Internal Variable Constitutive Equations for Isotropic Elasto-viscoplasticity," *International Journal of Plasticity*, Vol. 5, pp. 521~549.

Machand, A. and Duffy, J. W., 1988, "An Experimental Study of the Formation Process of Adiabatic Shear Bands in a Structural Steel," *Journal of the Mechanics and Physics of Solids*, Vol. 35, pp. 251~283.

Merzer, A. M., 1982, "Modelling of Adiabatic Shear Band Development from Small Imperfections," *Journal of the Mechanics and Physics of Solids*, Vol. 30, pp. 323~338.

Needleman, A., 1988, "Material Rate Dependence and Mesh Sensitivity in Localization Problems," *Computer Methods in Applied Mechanics and Engineering*, Vol. 67, pp. 69~85.

Wright, T. W. and Walter, J. W., 1987, "On Stress Collapse in Adiabatic Shear Bands," *Journal of the Mechanics and Physics of Solids*, Vol. 35, pp. 701~720.

Wright, T. W., 1987, "Steady Shearing in a Viscoplastic Solid," *Journal of the Mechanics and Physics of Solids*, Vol. 35, pp. 269~282.